Anomalous electric and magnetic properties of V_2O_3 in the metallic state

P. Hertel and J. Appel
I. Institut für Theoretische Physik, Universität Hamburg, D-2000 Hamburg 36, Federal Republic of Germany
(Received 4 March 1985)

Assuming the Hubbard model for the tightly bound a_{1g} electrons of the two pairs of V atoms within the unit cell of metallic V_2O_3, we have studied the correlated ground and excited molecular states. Using the exact wave functions of the singlet ground state and of the first excited triplet state, we evaluate the molecular magnetic susceptibility $\chi_0(\omega)$. The susceptibility of the conduction (e_g) electrons $\chi(\mathbf{q},\omega)$ is obtained in terms of χ_0 and the conduction-electron polarizability. The conduction-electron mass renormalization m^*/m_b is due to the virtual magnetic excitations of the a_{1g} electrons, introducing antiferromagnetic correlations between the V pairs. The resistivity $\rho=AT^2$ is caused by virtual exchange of these excitations. Both quantities are obtained from $\chi(\mathbf{q},\omega)$. The results are discussed in terms of the pertinent parameters in χ, such as the intra-atomic exchange interaction between the a_{1g} and e_g electrons, and are compared with the experimental results. Because the antiferromagnetic spin-fluctuation model does not account for the susceptibility enhancement at $q=0$ and because A is not sufficiently large we use Landau's Fermi-liquid theory to arrive at a consistent quasiparticle description of metallic V_2O_3. The Landau scattering parameters A_1 are obtained by applying the potential-scattering model for the quasiparticle interaction due to the molecular magnetic excitations. It is found that the experimental values for the specific heat, the static susceptibility, and the electrical resistivity can be explained in a consistent manner.

I. INTRODUCTION

Recently, the electric and magnetic properties of V_2O_3 have attracted the interest of experimentalists and theoreticians alike, to an extent that few other solids have. One reason for this interest is the attempt to understand the nature of the metal-insulator (M-I) transition at the temperature $T=150$ K. This transition is accompanied by an antiferromagnetic ordering with an unexpected number of Bohr magnetons per site ($1.2\mu_B$) for a V^{3+} configuration and by a monoclinic distortion of the trigonal structure. The second reason for the interest in V_2O_3 is to understand the anomalous behavior of the metallic state, due to some kind of spin-fluctuation effect.[1-15]

The basic question with regard to the M-I transition, as it emerged in the following years, is the following: What exactly is the type of electron-electron exchange-correlation effect that dominates the M-I transition and how is it to be formulated? The Brinkman-Rice (BR) theory[8,9] of conduction electrons with short-range Coulombic interactions, and moving in narrow d bands, is based on Gutzwiller's treatment[7] of the Hubbard Hamiltonian. This theory predicts a metal-insulator transition as the intra-atomic Coulomb interaction is increased beyond a critical interaction, the value of which depends on the filling of the conduction band. As for the metallic state, the Hall effect should be strongly temperature dependent near the M-I transition because of the change in the quasiparticle distribution as the M-I transition is approached and the electrons tend to become localized. Such a change has not been observed (McWhan *et al.*[16]; J. Honig[17]). The BR theory yields for the metallic phase a mass enhancement m^*/m_{band}, that is comparable to the susceptibility enhancement χ/χ_{Pauli}, whereas the observed χ enhancement is about twice that of m^*. This enhancement ratio is, however, much less than that one might expect from the ordinary paramagnon theory. Finally, Castellani *et al.*[13,14] claim that in the BR model the expression for the mass enhancement, when evaluated for a realistic set of parameter values for V_2O_3, gives an enhancement that is insufficient to account for the observed ratio $m^*/m\simeq 5$. In summary, it appears that the electrons in V_2O_3 are not the original BR Fermi liquid that is close to a localization transition, as is the case for normal ^{3}He (Ref. 18) below the Fermi temperature.

There are two other theoretical approaches—by Castellani, Natoli, and Ranninger[13,14] and by Ashkenazi and Weger[6]—both of which are based on a Hubbard-like Hamiltonian. These authors use realistic electronic parameters, as they are obtained from band-structure calculations. The model Hamiltonians are treated in the unrestricted Hartree-Fock approximation. Both groups, however, are mainly interested in the insulating phase and in the metal-to-insulator transition; they do not evaluate the metallic properties of V_2O_3 (see Fig. 1). Castellani *et al.*[15] give some qualitative arguments in favor of spin-fluctuation (paramagnon) effects in the metallic phase that lead to a Stoner enhancement of the Pauli susceptibility and to a large effective mass. Without giving details, the authors also point toward the importance of short-ranged spin correlations within the vertical pairs of V atoms oriented along the c axis. Likewise, in their "excitonic" model, Ashkenazi and Weger emphasize the importance of the V-atom pairs and also the role of the two types of electrons, a_{1g} and e_g. They discuss the change of the c/a ratio at the transition and conclude that the change in distance between c-axis neighbors changes the nature of the a_{1g} band from delocalized to localized. The

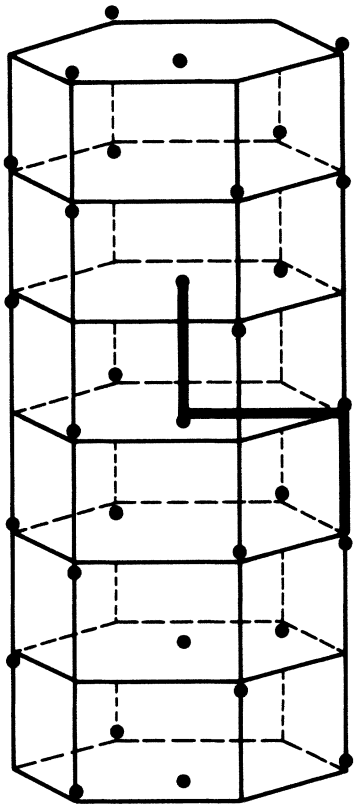

FIG. 1. Hexagonal unit cell of V_2O_3 in the trigonal metallic state.

localization of the a_{1g} electrons also causes, via the atomic exchange interaction, the localization of the e_g electrons. This localization, then, causes the material to become insulating. We believe, based on the following discussion, that the M-I transition is a magnetic transition driven by a rather weak exchange interaction between electrons at different parts of the Fermi surface (i.e., a type of nesting transition as it occurs in chromium[19–21]), resulting also in a localization of the e_g electrons below the metal-insulator transition.

The M-I transition can be suppressed by applying pressure; thereby, the metallic phase of V_2O_3 persists down to 0.3 K.[22] The anomalous metallic behavior is of particular interest since it shows the inherent electron correlation effects that tend to drive the system into the antiferromagnetic insulating phase. Experimentally, these effects manifest themselves in a large renormalization of the electron density of states at the Fermi surface. Firstly, measurements of the electronic heat capacity[22,23] show that the electronic specific heat in the metallic phase is extremely large, $\gamma \approx 32$ mJ/K^2 mol V (the uncertainty in γ is high, $\sim 20\%$), and leads to a value of 6.7 states/(eV V-atom spin). Hence $N^*(\varepsilon_F)/N_{\text{band}}(\varepsilon_F) \sim 5$,[22] if one takes the value $N_{\text{band}}(\varepsilon_F) = 1.5$ states/(eV V-atom spin), found by different authors.[6,14,24] Secondly, from the measurements of the paramagnetic susceptibility[25,26] of 1.84×10^{-3} emu per mole of V_2O_3 near the transition, one finds an effective density of states, $N_\chi(\varepsilon_F) \sim 14$ states/(eV V-atom spin) corresponding to an enhancement of ~ 12. A third unusual behavior is found in experimental studies of transport properties which show an unusually large T^2 term in the electrical resistivity, $\rho - \rho_0 = 0.042\,T^2$,[22,27] in units of $\mu\Omega$ cm and T in degrees kelvin. Only the heavy fermion metals have larger T^2 coefficients, $A_{CeAl_3} \simeq 30$.[28] By virtue of this anomalous behavior, the question arises as to why metallic V_2O_3 does not exhibit some kind of anisotropic superconductivity, perhaps triplet superconductivity, as recently pointed out by Anderson.[29] In 1969 Mott[30] suggested that BCS superconductivity may not occur because the metal atoms carry residual magnetic moments. It is also possible that the metallic phase of stochiometric V_2O_3 orders antiferromagnetically at sufficiently low temperatures,[31] which does not necessarily exclude the possibility of superconductivity.

In this paper we address the anomalous metallic behavior of V_2O_3, and not the M-I transition. We rely upon some recent theoretical work about the electronic structure of V_2O_3.[14,24,32] There are two different types of $3d$ electrons. The vanadium $3d$-t_{2g} band decomposes in the trigonal symmetry of a metal site into two different bands, for a_{1g} and e_g electrons, both of which incorporate ligand admixtures. The a_{1g} electrons tend to form covalent molecular bonds between vertical V pairs by virtue of a larger overlap integral along the c axis and a small overlap integral between neighbors perpendicular to the c axis. The nondegenerate a_{1g} bonding band can accommodate two electrons per unit cell, containing two pairs of V atoms (Fig. 2). This band is the lower of the two bands originating from the splitting of the a_{1g} band for a simple V_2 pair when proceeding to the actual trigonal unit cell containing two V_2 pairs. The Fermi energy ε_F is located in the well of a double peak caused by this splitting. Thus

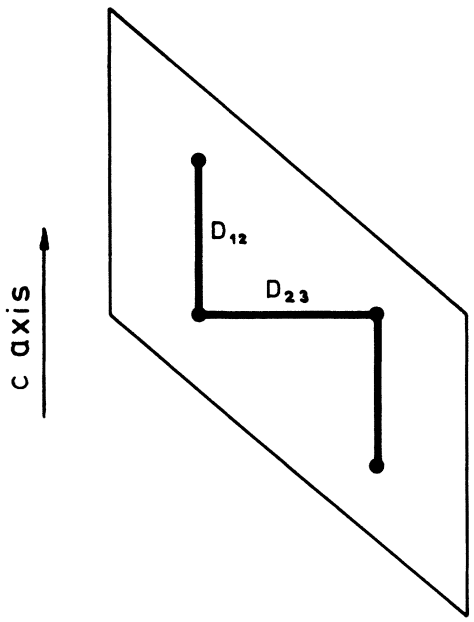

FIG. 2. Schematic illustration of the positions of the four V atoms within the unit cell. D_{12} gives the distance between the two V atoms in the vertical pair; D_{23} gives the distance between the two V atoms of the horizontal pairs.

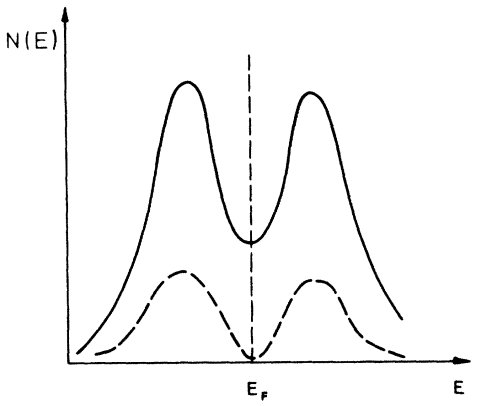

FIG. 3. Sketch of the density of states. Plotted are the partial densities of the a_{1g} electrons (— — —) and of the e_g electrons (——).

below ε_F there is $\frac{1}{2}$ a_{1g} electron per V atom (cf. Fig. 3).

Altogether we must accommodate two d electrons per V atom in the conduction bands. That leaves $\frac{3}{2}$ electrons per V atom for the doubly degenerate e_g bonding band. Here the splitting of the band—when proceeding from two to four V atoms in the unit cell—is not so large as to separate the split-off subbands. There is substantial overlap. The Fermi energy falls into a region with a high density of e_g states and, therefore, the thermodynamic and transport properties of metallic V_2O_3 are governed by e_g electrons.

In the following we attribute the anomalous metallic behavior of V_2O_3 to that of the e_g electrons caused by local, molecular magnetic excitations of the a_{1g} electrons. To this end, we treat the e_g electrons as being nearly-free-electron-like. Their interaction with the molecular excitations of the a_{1g} electrons causes the mass enhancement and the paramagnetic susceptibility enhancement; these local excitations also mediate an indirect interaction between the e_g electrons resulting in the T^2 dependence of the resistivity.

II. ELECTRON MODEL FOR V_2O_3

As already stated in the Introduction, any realistic approach to the metallic phase of V_2O_3 must take into account the two different bands, a_{1g} and e_g, near the Fermi level. Here, we adopt a simplified model in that we treat the e_g electrons as free-electron-like with 1.5 electrons per V-atom within the doubly degenerate band. This number is obtained from band-structure calculations.[24,32] Then there are 0.5 electrons per V-atom left for the a_{1g} band. Since the latter do not significantly contribute to the density of states at the Fermi level, we describe these electrons in terms of many-electron eigenstates of the molecular Hamiltonian for four vanadium atoms,

$$H_{\rm mol}=t\sum_{\sigma,\alpha=1,}^{4}a^{\dagger}_{\alpha\sigma}a_{\alpha\sigma}-a\sum_{\sigma}(a^{\dagger}_{1\sigma}a_{2\sigma}+a^{\dagger}_{2\sigma}a_{1\sigma}+a^{\dagger}_{3\sigma}a_{4\sigma}+a^{\dagger}_{4\sigma}a_{3\sigma})$$
$$-b\sum_{\sigma}(a^{\dagger}_{2\sigma}a_{3\sigma}+a^{\dagger}_{3\sigma}a_{2\sigma}+a^{\dagger}_{4\sigma}a_{1\sigma}+a^{\dagger}_{1\sigma}a_{4\sigma})+U\sum_{\alpha=1}^{4}n_{\alpha\uparrow}n_{\alpha\downarrow}\ . \tag{1}$$

Here the a_α ($\alpha=1,2,3,4$) are the annihilation operators of the Wannier states which transform according to the one-dimensional representation a_{1g} at the four V sites α within the unit cell. The quantity a is the transfer integral between neighbors along the c axis and has a large value compared to the transfer integral b between neighbors perpendicular to the c axis; U is the Coulomb repulsion between electrons in the same orbit. In order to be consistent with the periodicity of the crystal, we have closed the molecule, consisting of the four vanadium atoms in the unit cell, by periodic boundary conditions. By using this procedure we neglect the dispersion of the a_{1g} band and take the $k=0$ point as being representative for the center of gravity of the a_{1g} band. One pertinent advantage of the molecular approach is that we can take into account the electron correlation effects. Since in the average there are exactly two a_{1g} electrons at the molecule (unit cell), we solve Eq. (1) with the fixed $n=2$ occupancy for the molecule. An analogous problem with two atoms within the molecule has been solved by Falicov.[33]

The ground state which is a spin-singlet state may be written as the linear combination

$$\psi=\sum_{i=1}^{4}\eta_i\phi_i\ , \tag{2}$$

consisting of the following many-electron wave functions:

$$\phi_1=\tfrac{1}{2}\sum_{\alpha=1}^{4}a^{\dagger}_{\alpha\uparrow}a^{\dagger}_{\alpha\downarrow}|0\rangle\ ,$$
$$\phi_2=\tfrac{1}{2}(a^{\dagger}_{1\uparrow}a^{\dagger}_{2\downarrow}+a^{\dagger}_{2\uparrow}a^{\dagger}_{1\downarrow}+a^{\dagger}_{3\uparrow}a^{\dagger}_{4\downarrow}+a^{\dagger}_{4\uparrow}a^{\dagger}_{3\downarrow})|0\rangle\ ,$$
$$\phi_3=\tfrac{1}{2}(a^{\dagger}_{2\uparrow}a^{\dagger}_{3\downarrow}+a^{\dagger}_{3\uparrow}a^{\dagger}_{2\downarrow}+a^{\dagger}_{4\uparrow}a^{\dagger}_{1\downarrow}+a^{\dagger}_{1\uparrow}a_{1\uparrow}a^{\dagger}_{4\downarrow})|0\rangle\ , \tag{3}$$
$$\phi_4=\tfrac{1}{2}(a^{\dagger}_{1\uparrow}a^{\dagger}_{3\downarrow}+a^{\dagger}_{3\uparrow}a^{\dagger}_{1\downarrow}+a^{\dagger}_{2\uparrow}a^{\dagger}_{4\downarrow}+a^{\dagger}_{4\uparrow}a^{\dagger}_{2\downarrow})|0\rangle\ .$$

By applying the Hamiltonian, Eq. (1), to the ϕ_i, we obtain the following secular equation:

$$\begin{bmatrix}-E+(2t+U) & -2a & -2b & 0\\ -2a & -E+2t & 0 & -2b\\ -2b & 0 & -E+2t & -2a\\ 0 & -2b & -2a & -E+2t\end{bmatrix}\begin{bmatrix}\phi_1\\ \phi_2\\ \phi_3\\ \phi_4\end{bmatrix}=0\ . \tag{4}$$

From this equation we evaluate numerically the ground-state energy E_S and the associated eigenvectors η_i in terms of the parameters a,b,U. Furthermore, this equation yields three other singlet states (cf. Appendix A). The first-excited state is a spin-triplet state with the ener-

gy $E_T=-2a$. The wave functions are

$$\psi_{T_1}=\tfrac{1}{2}(a_{1\uparrow}^{\dagger}+a_{2\uparrow}^{\dagger})(a_{3\uparrow}^{\dagger}+a_{4\uparrow}^{\dagger})\,|\,0\rangle\ ,$$

$$\psi_{T_0}=\frac{1}{2\sqrt{2}}[(a_{1\uparrow}^{\dagger}+a_{2\uparrow}^{\dagger})(a_{3\downarrow}^{\dagger}+a_{4\downarrow}^{\dagger})+(a_{1\downarrow}^{\dagger}+a_{2\downarrow}^{\dagger})(a_{3\uparrow}^{\dagger}+a_{4\uparrow}^{\dagger})]\,|\,0\rangle\ , \tag{5}$$

$$\psi_{T_{-1}}=\tfrac{1}{2}(a_{1\downarrow}^{\dagger}+a_{2\downarrow}^{\dagger})(a_{3\downarrow}^{\dagger}+a_{4\downarrow}^{\dagger})\,|\,0\rangle\ .$$

The other excited states (altogether there are 28 states) are easily obtained by appropriate linear combinations of the form of Eqs. (1) and (5) and are given in Appendix A. However, the other states have much higher energies and, hence, they are neglected in the following. For example, for the values of the parameters, $U=1.5$ eV, $a=0.65$ eV, and $b=0.15$ eV, which are typical for V_2O_3,[3] the ground-state energy is -1.43 eV and the energy of the first-excited triplet state is -1.3 eV, whereas the energy of the next-higher state, being a singlet, is -0.85 eV and, hence, is much higher.

In order to study the magnetic properties of V_2O_3, it is pertinent to consider the spin correlations within the molecule. By assuming that all spins are quantized along the c axis, $\mathbf{S}_\alpha$ is given by $S_\alpha=n_{\alpha\uparrow}-n_{\alpha\downarrow}$. In the ground state, we find, for the above-mentioned parameters, the following spin correlations:

$$\langle S_1S_2\rangle=\langle S_3S_4\rangle=-\tfrac{1}{2}\eta_1^2=-0.055\ ,$$

$$\langle S_1S_3\rangle=\langle S_2S_4\rangle=-\tfrac{1}{2}\eta_3^2=-0.21\ ,$$

$$\langle S_1S_4\rangle=\langle S_2S_3\rangle=-\tfrac{1}{2}\eta_2^2=-0.2\ ,$$

whereas for the triplet state we obtain

$$\langle S_1S_2\rangle=\langle S_3S_4\rangle=0\ ,$$

$$\langle S_1S_3\rangle=\langle S_1S_4\rangle=\langle S_2S_3\rangle=\langle S_2S_4\rangle=-\tfrac{1}{4}\ .$$

From these values we conclude that in the ground state there is a strong antiferromagnetic correlation between spins on different c-axis neighbor pairs and a relatively small correlation between the spins of a c-axis pair. In the triplet state there is no spin correlation between the spins of one c-axis pair and a small correlation between different pairs. This is one reason for the tendency towards antiferromagnetic ordering between neighbors within the plane perpendicular to the c axis.

Turning now to the coupled e_g-a_{1g} electron system, we assume that the Fermi level is shifted by the crystal field so that it falls in between the singlet and the triplet state. For the interaction between the two kinds of electrons, we assume an intra-atomic Coulomb-exchange interaction,

$$\begin{aligned}H_{\rm int}&=-J\sum_{n,\alpha}\mathbf{S}_{n\alpha}\cdot\boldsymbol{\sigma}(\mathbf{R}_{n\alpha})\\&=-J\sum_{n,\alpha}[S_{n\alpha}^{z}(c_{n\alpha\uparrow}^{\dagger}c_{n\alpha\uparrow}-c_{n\alpha\downarrow}^{\dagger}c_{n\alpha\downarrow})\\&\quad+S_{n\alpha}^{+}c_{n\alpha\downarrow}^{\dagger}c_{n\alpha\uparrow}+S_{n\alpha}^{-}c_{n\alpha\uparrow}^{\dagger}c_{n\alpha\downarrow}]\ ,\end{aligned} \tag{6}$$

where, in the tight-binding picture, the $c_{n\alpha}$ are the annihilation operators at the nth unit cell and the site α within the unit cell. The $S_{n\alpha}$ are the spin operators of the a_{1g} electrons, and the σ operators are those of the conduction electrons. The exchange integral is given by

$$\begin{aligned}J=-\int d^3r_1\int d^3r_2\,\psi_{a_{1g}}(\mathbf{r}_2-\mathbf{R}_{n\alpha})&\\\times\psi_{e_g}(\mathbf{r}_1-\mathbf{R}_{n\alpha})\frac{e^2}{|\mathbf{r}_1-\mathbf{r}_2|}&\\\times\psi_{a_{1g}}(\mathbf{r}_1-\mathbf{R}_{n\alpha})\psi_{e_g}(\mathbf{r}_2-\mathbf{R}_{n\alpha})\ .&\end{aligned} \tag{7}$$

We assume that J—which is independent of $\mathbf{R}_{n\alpha}$— is a constant, i.e., independent of energy. By Fourier-transforming the conduction-electron states into the $\mathbf{k}$ representation,

$$c_{n\alpha}=\frac{1}{(4N_c)^{1/2}}\sum_{\mathbf{k}}e^{i\mathbf{k}\cdot\mathbf{R}_{n\alpha}}c_{\mathbf{k}}\ , \tag{8}$$

where N_c is the number of unit cells, we obtain the interacting part of the Hamiltonian,

$$\begin{aligned}H_{\rm int}=-\frac{J}{4N_c}\sum_{\mathbf{k},\mathbf{q},n\alpha}e^{-i\mathbf{q}\cdot\mathbf{R}_{n\alpha}}&\\\times[S_{n\alpha}^{z}(c_{\mathbf{k}+\mathbf{q}\uparrow}^{\dagger}c_{\mathbf{k}\uparrow}-c_{\mathbf{k}+\mathbf{q}\downarrow}^{\dagger}c_{\mathbf{k}\downarrow})&\\+S_{n\alpha}^{+}c_{\mathbf{k}+\mathbf{q}\downarrow}^{\dagger}c_{\mathbf{k}\uparrow}+S_{n\alpha}^{-}c_{\mathbf{k}+\mathbf{q}\uparrow}^{\dagger}c_{\mathbf{k}\uparrow}]\ .&\end{aligned} \tag{9}$$

This interaction is added to the free-electron Hamiltonian for the conduction (e_g) electrons and the Hamiltonian, Eq. (1), for the a_{1g} electrons.

III. SPIN SUSCEPTIBILITY, ELECTRON MASS ENHANCEMENT, AND ELECTRICAL RESISTIVITY

In this section we evaluate the transverse dynamic spin susceptibility χ of the coupled a_{1g}-e_g electron systems. First, we find the molecular susceptibility χ_0 of the a_{1g} electrons localized at the molecule that consists of the four vanadium atoms within the trigonal unit cell, cf. Fig. 2. Then, we proceed to evaluate χ in terms of χ_0 and χ^e, the latter being the susceptibility of the free-electron-like e_g electrons.

In order to calculate the molecular susceptibility,

$$(\chi_0^{+-})_{\alpha\beta}=-i\Theta(t)\langle\langle[S_{n\alpha}^{+}(t),S_{n'\beta}^{-}]\rangle\rangle\ , \tag{10}$$

we start from the spectral representation,

$$(\chi_0^{+-})_{\alpha\beta}=-\frac{1}{\sum_i e^{-\beta E_i}}\sum_{i,j}(e^{-\beta E_i}-e^{-\beta E_j})\times\frac{\langle i\,|\,S_{n\alpha}^{+}\,|\,j\rangle\langle j\,|\,S_{n\beta}^{-}\,|\,i\rangle}{\omega-(E_j-E_i)+i\delta}\ . \tag{11}$$

Here, i denotes the molecular states discussed in Sec. II. We assume the molecules to be independent of one another and, therefore, terms with $n\neq n'$ do not exist. Taking

into account only the singlet ground state and the first-excited triplet state—all other states are much higher in energy and do not play a significant role at low temperatures—we get

$$(\chi_0^{+-})_{\alpha\beta}=-M_{\alpha\beta}\frac{1-e^{-\beta\Delta}}{1+3e^{-\beta\Delta}}\frac{2\Delta}{\omega^2-\Delta^2+2ii\delta\omega} . \quad (12)$$

Here, Δ is the singlet-to-triplet separation; $M_{\alpha\beta}$ is given by

$$M_{\alpha\beta}=\langle S\,|\,S_\alpha^+\,|\,T\rangle\langle T\,|\,S_\beta^-\,|\,S\rangle = [\tfrac{1}{4}(\eta_1+\eta_2)]^2\begin{vmatrix} 1 & 1 & -1 & -1 \\ 1 & 1 & -1 & -1 \\ -1 & -1 & 1 & 1 \\ -1 & -1 & 1 & 1 \end{vmatrix} , \quad (13)$$

where S stands for singlet and T for triplet. In the limit $T\to 0$ we obtain

$$(\chi_0^{+-})_{\alpha\beta}=-M_{\alpha\beta}\frac{2\Delta}{\omega^2-\Delta^2+2i\delta\omega}\equiv M_{\alpha\beta}\chi_0(\omega) . \quad (14)$$

Apart from the fact that here $(\chi_0^{+-})_{\alpha\beta}$ is a matrix due to the molecular structure of the excitations, there exists some analogy to the $4f$ magnetic excitons in rare-earth metals which have been invented by White and Fulde to explain the conduction-electron mass enhancement in praseodymium.[34] Within the random-phase approximation (RPA) the transverse susceptibility of the coupled a_{1g}-e_g electron systems is evaluated according to the diagram of Fig. 4. We obtain

$$\chi^{+-}_{n\alpha n'\alpha'}(\omega)=[\chi_0^{+-}(\omega)]_{n\alpha n'\alpha'} + \sum_{n_1,\alpha_1,n_2,\alpha_2}[\chi_0(\omega)]_{n\alpha n_1\alpha_1} \times J^2\chi^e_{n_1\alpha_1 n_2\alpha_2}(\omega)\chi^{+-}_{n_2\alpha_2 n'\alpha'}(\omega) , \quad (15)$$

where χ_0 is the polarizability of the a_{1g} electrons, cf. Eq. (14), and χ^e is the polarizability of the conduction electrons.

Using the equation

$$(\chi_0^{+-})_{n\alpha'\alpha'}=\delta_{nn'}M_{\alpha\alpha'}\chi_0(\omega) , \quad (16)$$

and using the Fourier transform

$$\chi^{+-}_{n\alpha n'\alpha'}=\frac{1}{4N_c}\sum_{\mathbf{q}}e^{i\mathbf{q}\cdot(\mathbf{R}_n+\tau_\alpha-\mathbf{R}_{n'}-\tau_{\alpha'})}\chi^{+-}(\mathbf{q}) , \quad (17)$$

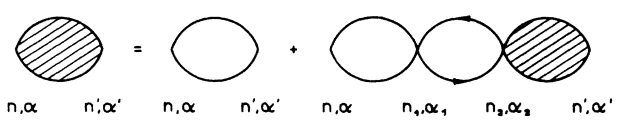

FIG. 4. Diagrams for the evaluation of the conduction-electron susceptibility χ^{+-}; χ_0 and χ^e represent the molecular susceptibility (singlet-triplet excitations) and the free-electron polarizability, respectively.

we obtain

$$\chi^{+-}(\mathbf{q},\omega)=M(\mathbf{q})\chi_0(\omega)+J^2\chi_0(\omega)M(\mathbf{q})\chi^e(\mathbf{q},\omega)\chi^{+-}(\mathbf{q},\omega). \quad (18)$$

In Eq. (17), the τ_α are the basis vectors within the unit cell and $M(\mathbf{q})$, Eq. (18), is

$$M(\mathbf{q})=\tfrac{1}{4}\sum_{\alpha,\beta=1}^{4}e^{-i\mathbf{q}\cdot\tau_\alpha}M_{\alpha\beta}e^{i\mathbf{q}\cdot\tau_\beta} . \quad (19)$$

The function

$$\chi^e(q,\omega)=\frac{g}{4N_c}\sum_{\mathbf{p}}\frac{f_{\mathbf{p}+\mathbf{q}}-f_{\mathbf{p}}}{\omega-\varepsilon(\mathbf{p}+\mathbf{q})+\varepsilon(\mathbf{p})+i\delta} \quad (20)$$

is the Lindhard function; $g=2$ is the degeneracy factor of the e_g band. Equation (18) is solved by

$$\chi^{+-}(\mathbf{q},\omega)=\frac{\chi_0(\omega)M(\mathbf{q})}{1-J^2\chi_0(\omega)M(\mathbf{q})\chi^e(\mathbf{q},\omega)} . \quad (21)$$

The longitudinal susceptibility is defined by the equation

$$\chi^l(\mathbf{q},\omega)=-i\Theta(t)\langle\langle[S^z_{n\alpha}(t),S^z_{n'\beta'}(0)]\rangle\rangle , \quad (22)$$

and we obtain

$$\chi^l(\mathbf{q},\omega)=\frac{\frac{1}{2}\chi_0(\omega)M(\mathbf{q})}{1-J^2\chi_0(\omega)M(\mathbf{q})\chi^e(\mathbf{q},\omega)} . \quad (23)$$

This form of the susceptibility function, Eqs. (21) and (23), indicates what type of magnetic structure could arise from a phase transition where the susceptibilities go to ∞, i.e., the common denominator vanishes. The quantity $M(\mathbf{q})$ of the denominator in our model is given by

$$M(\mathbf{q})=\tfrac{1}{4}(\eta_1+\eta_2)^2\left[\cos\left[\frac{q_z d_{12}}{2}\right]\times\sin\left[\frac{q_x d_{23}}{2}-\frac{q_z d_{12}}{2}\right]\right]^2 . \quad (24)$$

Here, d_{12} is the distance between two V atoms of the pairs oriented parallel to the c axis, whereas d_{23} is the distance between two V atoms of the pairs perpendicular to the c axis, Fig. 2. The function $\chi^e(q,0)$ is the static Lindhard function, and is a slowly varying function of q when compared with $M(\mathbf{q})$. Hence, the maximum of the susceptibility is determined by the maximum of $M(\mathbf{q})$, obtained for $q_z=0$ and $q_x=\pi/d_{23}$. Thus the magnetic ordering due to the "freezing" of spin-wave excitations is antiferromagnetic perpendicular to the c axis and ferromagnetic parallel to the c axis, in agreement with experimental findings. This magnetic structure is found by elastic-neutron-scattering experiments in the insulating phase.[35] The magnitude of the saturation moment in

stoichiometric V_2O_3 was determined to be $1.2\mu_B$. No completely satisfactory explanation for this unusual moment has yet evolved. However, we would like to point out the fact that antiferromagnetic ordering, with an effective moment $\mu_B \simeq 0.5$, occurs even within the metallic phase in oxygen-rich V_2O_3.[35] These observations suggest that the a_{1g} electrons can order antiferromagnetically in the metallic state of V_2O_3.

Given the susceptibility, Eqs. (21) and (23), we can proceed to calculate the e_g-electron self-energy (see Fig. 5). The contribution of the transverse susceptibility to the self-energy is given by

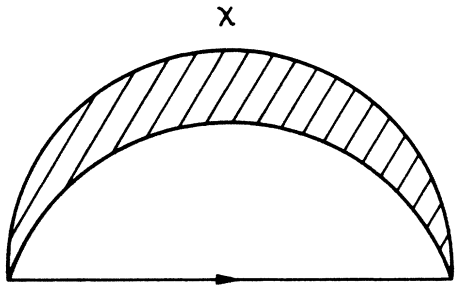

FIG. 5. Contribution of the exchange of the magnetic excitations to the conduction-electron self-energy.

$$\Sigma(\mathbf{p},\omega)=J^2\int_0^\infty \frac{d\omega'}{\pi}\int \frac{d^3p'}{(2\pi)^3}\mathrm{Im}\chi^{+-}(\mathbf{p}-\mathbf{p}',\omega')\left[\frac{f(\varepsilon(\mathbf{p}'))}{\omega+\omega'-\varepsilon(\mathbf{p}')}+\frac{1-f(\varepsilon(\mathbf{p}'))}{\omega-\omega'-\varepsilon(\mathbf{p}')}\right]. \tag{25}$$

By taking into account both the longitudinal and transverse magnetic excitations, and by performing the spin summation, we find that the shift in the specific heat due to the magnetic excitations in the limit of low temperatures is given by

$$\Delta C_v = T\frac{\partial \Delta S}{\partial T} = -Tk_B^2\pi^2 N(0)\int \frac{d\Omega}{4\pi}\left[\frac{\partial}{\partial\omega}\Sigma(\mathbf{p}_F,\omega)\right]_{\omega=0}. \tag{26}$$

Here, $N(0)=m_b p_F/\pi^2$ is the density of states per spin for the doubly degenerated e_g band. For the effective mass enhancement (cf. Appendix B for the details) we obtain

$$\frac{m^*}{m_b}-1=-3\int\frac{d\Omega}{4\pi}\left[\frac{\partial}{\partial\omega}\Sigma(\mathbf{p}_F,\omega)\right]$$

$$=\frac{3}{4\pi}\int d^3q\,\Theta(1-q)\chi^{+-}(\mathbf{q})\frac{1}{q}. \tag{27}$$

To evaluate this expression as a function of the dimensionless parameter

$$W=\tfrac{1}{4}(\eta_1+\eta_2)^2J^2N(0)\chi_0(0),$$

we take two slightly different approaches in averaging over the anisotropy of $\chi^{+-}(\mathbf{q})$. In the first case we take the Lindhard polarization function $\chi^e(q)$, which slowly varies with q, as compared with the function $M(\mathbf{q})$, to be a constant: $\chi=\chi_c(q_m)$. Here the wave vector q_m is defined by the maximum value of $M(\mathbf{q})$. The largest value which the parameter W can assume is, then, given by $W_0=1/\chi_c=1.148075$. For this case we show in Fig. 6 the effective mass enhancement m^*/m_b-1 as function of W. Near $W=W_0$, m^*/m_b-1 diverges logarithmically. In the second approach we generalize the planar model to the more realistic cylindrical symmetry. We take into account that every V atom of a c-axis pair "sees" three equivalent neighbor atoms in the plane perpendicular to the c axis (cf. Fig. 1). In other words, we take into account that another unit cell can be chosen by rotating the original cell about the c axis by an angle of 120° or 240°. The simplest way to account for the cylindrical symmetry is to replace the q_x vector in $M(\mathbf{q})$, Eq. (24), by the radius vector $q_\perp$, oriented perpendicular to the c axis. By allowing χ^e to be q dependent, we find that the maximum of the function $\chi^e(q)M(q)$ has shifted to a slightly smaller value of q compared to q_m, and the largest value of W is now given by $W_0=1.128\,682\,865\,5$. Because of the cylindrical symmetry of this model, the azimuth-angle integration in Eq. (27) can be performed. The resulting two-dimensional integral is shown as a function of W in Fig. 7. Again we find the logarithmic divergence at $W=W_0$.

The T^2 term of the electrical resistivity is derived elsewhere[36] by using the variational method,

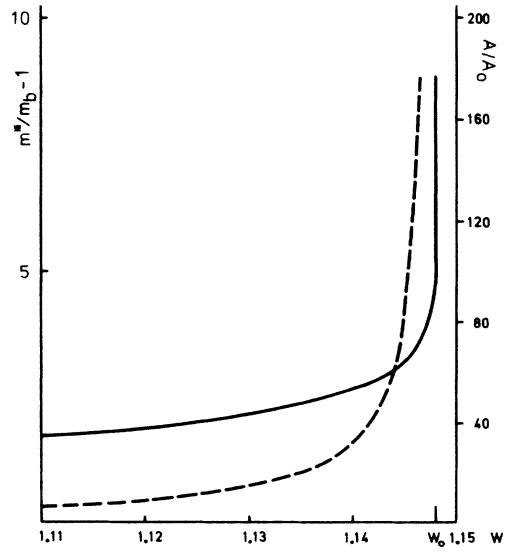

FIG. 6. Electronic mass enhancement m^*/m_b and electrical resistivity enhancement A/A_0 ($A_0=4.3\times10^{-5}$ $\mu\Omega\,\mathrm{cm/K^2}$) vs the strength of the effective interaction parameter W for χ^e independent of q.

$$\rho=\frac{1}{6k_BT}g\times 3\int\frac{d^3k'}{(2\pi)^3}\int\frac{d^3k'}{(2\pi)^3}[v(\mathbf{k}')-v(\mathbf{k})]^2U(\mathbf{k},\mathbf{k}')\left[\frac{2}{3}e\int\frac{d^3k}{(2\pi)^3}\mathbf{v}\frac{\partial f(\varepsilon)}{\partial\varepsilon}\right]^{-2}. \tag{28}$$

Here the transition rate is given by

$$U(\mathbf{k},\mathbf{k}')=I^2\int d^3q\,\delta(\mathbf{k}'-\mathbf{k}-\mathbf{q})\int_{-\infty}^{+\infty}\frac{d\Omega}{\pi}\mathrm{Im}\chi^{+-}(\mathbf{q},\Omega)\pi\delta(\varepsilon_{\mathbf{k}'}-\varepsilon_{\mathbf{k}}+\Omega)n(\Omega)[1-f(\varepsilon_{\mathbf{k}'})]f(\varepsilon_{\mathbf{k}'}). \tag{29}$$

In Eq. (28), $g=2$ is the band-degeneracy factor and the factor 3 in front of the integral in Eq. (28) arises from the spin summation that arises from the different contributions of the transverse and longitudinal magnetic excitations. Performing a momentum integration, we get

$$\rho=\frac{9\pi^3m_bJ^2}{4e^2p_F^6k_BT}\int\frac{d^3q}{(2\pi)^3}\Theta(1-q/2p_F)\int_{-\infty}^{+\infty}\frac{d\Omega}{\pi}q\,\mathrm{Im}\chi^{+-}(\mathbf{q},\Omega)\frac{\Omega}{1-e^{-\beta\Omega}}n(\Omega). \tag{30}$$

In the limit of low temperatures this expression becomes

$$\rho=\left[\frac{3\pi^4m_b^2J^2k_B^2}{2e^2p_F^6}\int\frac{d^3q}{(2\pi)^3}\Theta(1-q/2p_F)q\lim_{\Omega\to 0}\left[\frac{\mathrm{Im}\chi^{+-}(q,\Omega)}{\Omega}\right]\right]T^2=AT^2. \tag{31}$$

In Figs. 6 and Fig. 7 we plot A as a function of the parameter W for planar and the cylindrical models, respectively. In both cases, A rapidly increases with W, i.e., the strength of the exchange interaction J between a_{1g} and e_g electrons.

The measurement of the heat capacity yields, for the effective mass enhancement, $m^*/m_b\simeq 4.5$. To this mass ratio we fit the interaction parameter W with the results $W=1.146$ and $W=1.1237$ for the planar and cylindrical models, respectively. The values of W correspond to a value of about 0.1 eV for the interaction parameter J, which is a reasonable number. For the two W values the resistivity enhancement A/A_0 ($A_0=4.369\times 10^{-5}$ $\mu\Omega\,\mathrm{cm/K^2}$, as calculated from band-structure data) is found to be 150 and 50, respectively The resulting coefficients, $A=6.5\times 10^{-3}$ $\mu\Omega\,\mathrm{cm/K^2}$ and $A=2.18\times 10^{-3}$ $\mu\Omega\,\mathrm{cm/K^2}$, are 1 order of magnitude too small in comparison with the experimental result. Allowing for a larger mass enhancement, bearing in mind that the experimental value is known only up to an error of 20% leads to a somewhat improved agreement between theory and experiment. We mention that in A the Fermi momentum p_F is evaluated in the free-electron model, whereas the realistic band structure and the Fermi surface are not so simple. Allowing p_F to be a free parameter, the agreement of the resistivity coefficient A with the experimental value can be significantly improved, because of the strong dependence of A_0 on p_F. The shape of the Fermi surface and the effects of the band structure on the electron polarizability function $\chi^e(\mathbf{q})$ are important for the phase space of the singular region of the susceptibility χ^{+-}. In order to have a singular behavior of the effective mass enhancement and, hence, of A near a critical value W_0, we need a sufficiently large region in the q space where the denominator in the effective susceptibility is close to zero. For the two models discussed below Eq. (27), we have two different lines of singular behavior of χ^{+-} in $\mathbf{q}$ space. From Figs. 6 and 7 we conclude that the structure of the singular lines have a large influence on the enhancement factors. We also mention that the wave vector q_m where χ^{+-} reaches its maximum is determined by the structure of the electron polarizability χ^e. In conclusion, we find that the antiferromagnetic spin-fluctuation model in its present form is not yet sufficient to explain the metallic properties of V_2O_3 consistently for two pertinent reasons: The absolute value of the resistivity coefficient A is too small and, what proves to be the main deficiency, we have no explanation for the susceptibility enhancement at $q=0$.

Can we remedy these deficiencies? A comparison with rare-earth and actinide compounds[37–39]—e.g., $CeAl_3$, UB_{13}, UPt_3—suggests that we treat V_2O_3 as a heavy-electron Fermi liquid, as has recently been proposed by Anderson.[29] Just as V_2O_3, these compounds show a large mass and susceptibility enhancement and they have a very high resistivity coefficient. Both V_2O_3 and the compounds mentioned above have been treated as Brinkman-

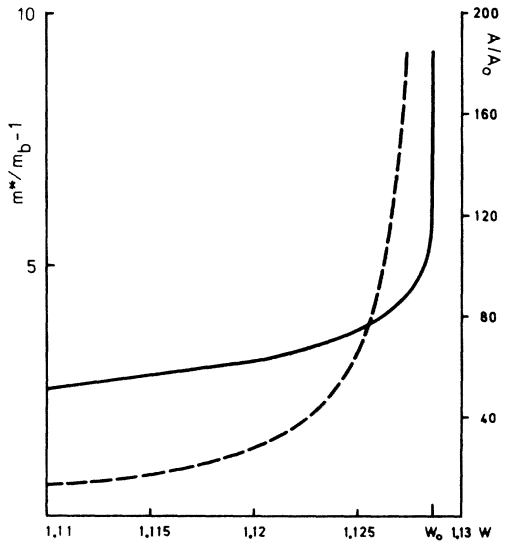

FIG. 7. Electronic mass enhancement m^*/m_b and electrical resistivity enhancement A/A_0 ($A_0=4.3\times 10^{-5}$ $\mu\Omega\,\mathrm{cm/K^2}$) vs the strength of the effective interaction parameter W for the cylindrically symmetric model.

Rice[7] Fermi liquids and are close to a paramagnetic or antimagnetic transition, as is ^{3}He. For these reasons, in the next section we treat V_2O_3 as a Fermi liquid. We first discuss the phenomenological Fermi-liquid model and attempt to fit the Landau parameters in a consistent manner. We then evaluate these parameters on a microscopic basis by using as the effective interaction a scattering potential which arises from the exchange of the collective modes, namely the molecular magnetic excitations of Sec. II.

IV. THE FERMI-LIQUID DESCRIPTION OF METALLIC V_2O_3

Landau's theory of Fermi liquids has been successfully applied to liquid ^{3}He. The properties of ^{3}He can be understood as those of a gas of quasiparticles if one assumes that the liquid is close to a phase transition where the instability is connected with the long-wavelength spin fluctuations occurring close to a ferromagnetic phase transition.[40–42] In addition, the transition is affected by the short-wavelength spin fluctuations occurring close to an antiferromagnetic transition.[43] The basic assumption is that both of the spin-fluctuation effects yield a quasiparticle scattering amplitude that is dominated by the exchange of collective modes in the two different particle-hole channels, in particular by the exchange of spin-density fluctuation[40] and rotons.[43] In addition, the density fluctuations are taken into account. These so-called potential-scattering models are appropriate for constructing the zero-frequency vertex function Γ^∞. The resulting scattering amplitude is then successfully used to compute the transport properties of ^{3}He. Hence, an important ingredient of the Fermi-liquid behavior is often a strong exchange interaction mediated by collective excitations.

As in the ^{3}He, there exists in V_2O_3—being close to an antiferromagnetic phase transition—a strong exchange interaction between the quasiparticles (i.e., the conduction electrons) due to the molecular magnetic excitations studied in Sec. III. This similarity suggest that we describe the metallic phase of V_2O_3 as a Fermi liquid, using our magnetic-excitation model.

We proceed by studying first the Fermi-liquid behavior in terms of the quasiparticle scattering amplitude, thereby assuming a potential-scattering model. In this phenomenological approach, we attempt to approximate the true scattering amplitude by adjustable parameters. Thereby, experimentally known quantities are used in determining the scattering amplitude in terms of a consistent parameter fit.

In the second part of this section we evaluate these parameters on the basis of a microscopic theory by using the magnetic excitation model for the spectral representation of the scattering potential.

Assuming that the scattering amplitude arises from the exchange of magnetic excitons we approximate the static vertex function Γ^∞ (i.e., first $\omega\to 0$, q being small, then $q/\omega\to\infty$) in the following manner, i.e., the potential-scattering model,

$$\Gamma^\infty(\mathbf{p}_1,\mathbf{p}_2,\mathbf{q})=-\sigma_{\alpha\gamma}(1)\cdot\sigma_{\beta\delta}(2)J(\mathbf{q}) +\sigma_{\alpha\delta}(1)\cdot\sigma_{\beta\gamma}(2)J(\mathbf{p}_2-\mathbf{p}_1-\mathbf{q}) . \quad (32)$$

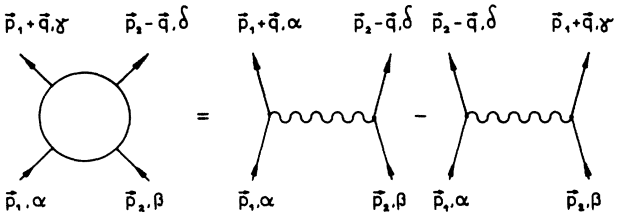

FIG. 8. Physical processes describing the potential-scattering model. The wavy line represents the exchanged antiferromagnetic spin fluctuations (magnetic singlet-triplet excitations).

In Fig. 8 the wavy line represents the propagator $J(\mathbf{q})$ for the exchange of a spin-density fluctuation. In the following we shall discuss $J(\mathbf{q})$ on the basis of our magnetic-excitation model; for the time being, however, we assume $J(\mathbf{q})$ to be any given potential. Since V_2O_3 is close to an antiferromagnetic phase transition, which implies the importance of short-wavelength spin-density fluctuations, we neglect the exchange of density fluctuations. The effect of these fluctuations is considered to be unimportant, in comparison with the exchange of the spin-density excitations.[44] Due to the formal similarity between the scattering amplitude for ordinary potential scattering through a local two-body interaction and the exchange of collective excitations we denote the approximation of the static vertex function as the potential-scattering model.

We assume, furthermore, that the Fermi surface of the conduction electrons is isotropic, which implies that because of the assumed Galilean invariance the effective potential depends only on the absolute value of the momentum transfer, q, for reasons of consistency. Since we are close to an antiferromagnetic phase transition, and since we have in mind the magnetic-excitation model governed by interband transitions (singlet-triplet excitations), the matrix elements for $q=0$ are equal to zero and, hence, we take $J(0)$ to be zero.

The quasiparticle scattering amplitude A is connected with the vertex function Γ^∞,

$$A(\mathbf{p}_1,\mathbf{p}_2,\mathbf{q})=N^*(\varepsilon_F)z_{\mathbf{p}_1}z_{\mathbf{p}_2}\Gamma^\infty(\mathbf{p}_1,\mathbf{p}_2,\mathbf{q}) . \quad (33)$$

The quantity N^* is the density of states of the quasiparticles and z is given by

$$z_{\mathbf{p}_1}=m_b/m^* , \quad (34)$$

where m_b is the band mass.

By eliminating the second pair of σ matrice in Eq. (32), we obtain

$$A(\mathbf{p}_1,\mathbf{p}_2,\mathbf{q})=N^*(\varepsilon_F)z^2\{\tfrac{3}{2}\delta_{\alpha\gamma}\delta_{\beta\gamma}J(q_1) -\sigma_{\alpha\gamma}(1)\sigma_{\beta\delta}(2)[J(q)+\tfrac{1}{2}J(q_1)]\} , \quad (35)$$

where

$$q=2p_F\sin(\theta/2)\sin(\phi/2) \quad (36)$$

and

$$q_1=|\mathbf{p}_2-\mathbf{p}_1-\mathbf{q}|=2p_F\sin(\theta/2)\cos(\phi/2) . \quad (37)$$

Here, θ is the angle between the two incoming particles and the scattering angle ϕ is the angle between the plane containing the incoming momenta and the plane containing the outgoing momenta.

From Eq. (35) we find the spin-symmetric and the spin-antisymmetric scattering amplitudes,

$$A^s(\theta,\phi)=\tfrac{3}{2}N^*(\varepsilon_F)z^2J(q_1)\ , \tag{38}$$

$$A^a(\theta,\phi)=-N^*(\varepsilon_F)z^2[J(q)+\tfrac{1}{2}J(q_1)]\ . \tag{39}$$

We note that A^s and A^a obey the sum rule for $\theta=0$:

$$A^s(\theta=0,\phi)+A^a(\theta=0,\phi)=0\ . \tag{40}$$

Furthermore, it is convenient to introduce the singlet and triplet scattering amplitudes,

$$A_{\rm sing}(\theta,\phi)=N^*(\varepsilon_F)z^2 3[J(q_1)+J(q)]\ , \tag{41}$$

$$A_{\rm trip}(\theta,\phi)=N^*(\varepsilon_F)z^2[J(q_1)-J(q)]\ . \tag{42}$$

In order to find the Landau parameters, we note that the Landau quasiparticle scattering amplitude $a(p_1,p_2)$ is related to the scattering amplitude A by the equation

$$a(\mathbf{p}_1,\mathbf{p}_2)=N^*(\varepsilon_F)^{-1}A(\theta,\phi=0)\ . \tag{43}$$

It is evident that knowledge of A goes beyond Landau theory, since A contains the full angular dependence of a scattering process.

The framework of the Landau Fermi-liquid theory can be extended to obtain the transport coefficients.[45] The low-temperature result for the thermal conductivity obtained by an exact solution of the Boltzmann equation is given by

$$\kappa=\frac{8\pi^2}{3}\frac{p_F^3}{(m^*)^4T}\frac{1}{\langle W(\theta,\phi)(1-\cos\theta)/\cos(\theta/2)\rangle}H(\lambda)\ , \tag{44}$$

where

$$H(\lambda)=\tfrac{1}{4}\sum_{n=0}^{\infty}\frac{(4n+5)(3-\lambda)}{(n+1)(2n+3)[(n+1)(2n+3)-\lambda]} \tag{45}$$

and

$$\lambda=\frac{\langle W(\theta,\phi)(1+2\cos\theta)/\cos(\theta/2)\rangle}{\langle W(\theta,\phi)/\cos(\theta/2)\rangle}\ . \tag{46}$$

Here the $\langle\cdots\rangle$ values are defined by the angular averages,

$$\langle F(\theta,\phi)\rangle\equiv\frac{1}{4\pi}\int_0^{2\pi}d\phi\int_0^{\pi}d\theta\sin\theta F(\theta,\phi)\ . \tag{47}$$

The quantity W is related to the scattering amplitude A,

$$W(\theta,\phi)=\frac{\pi}{\hbar}[N^*(\varepsilon_F)]^{-2}\{\tfrac{1}{4}[A_{\rm trip}(\theta,\phi)+A_{\rm sing}(\theta,\phi)]^2+\tfrac{1}{2}A_{\rm trip}^2(\theta,\phi)\}\ . \tag{48}$$

The electrical resistivity is obtained from the thermal conductivity via the Wiedemann-Franz law since we assume elastic scattering processes,

$$\frac{1}{\rho}=\sigma=\frac{3}{\pi^2}\left[\frac{e}{k_B}\right]^2\frac{1}{T}\kappa\ . \tag{49}$$

We parametrize the scattering polynomial by expanding J in terms of Legendre polynomials,

$$N^*(\varepsilon_F)z^2J=\sum_l J_lP_l\left[1-\frac{q^2}{2p_F^2}\right]\ . \tag{50}$$

Here,

$$J_l=\frac{2l+1}{2}\int_0^{2p_F}dq\frac{q}{p_F^2}P_l\left[1-\frac{q^2}{2p_F^2}\right]N^*(\varepsilon_F)z^2J(q)\ . \tag{51}$$

In order to find the Landau parameters, we use the result for the forward-scattering amplitude,

$$A^s(\theta,\phi=0)=\sum_l A_l^sP_l(\cos\theta)\ , \tag{52}$$

$$A^a(\theta,\phi=0)=\sum_l A_l^aP_l(\cos\theta)\ . \tag{53}$$

These expressions, together with Eqs. (38), (39), and Eq. (50), yield

$$A_l^s=\tfrac{3}{2}J_l\ , \tag{54}$$

$$A_l^a=-\tfrac{1}{2}J_l-\delta_{l,0}\sum_l J_l\ . \tag{55}$$

Since we assume $J(q=0)=0$, we get

$$\sum_l J_l=0\ . \tag{56}$$

Thereby, we immediately obtain, cf. Ref. 44,

$$A_l^a=-\tfrac{1}{3}A_l^s\ . \tag{57}$$

To evaluate the resistivity, the quantity $W(\theta,\phi)$ is parametrized by using Eqs. (41), (42), and (50). The result is

$$W(\theta,\phi)=\frac{\pi}{\hbar}[N^*(\varepsilon_F)]^{-2\frac{2}{3}}\times\sum_{l,l'}A_l^sA_{l'}^s\{2P_l(q_1)P_{l'}(q_1)+[P_l(q_1)+P_l(q)]\times[P_{l'}(q_1)+P_{l'}(q)]\}, \tag{58}$$

where

$$P_l(q)\equiv P_l\left[1-\frac{q^2}{2p_F^2}\right]\ .$$

The average values, Eq. (47), of the product of two Legendre polynomials, are readily evaluated. Using these averages, we parametrize the resistivity ρ in terms of the Landau coefficients A_l^s,

$$\rho=\frac{\pi^5(m^*)^2k_B^2}{\hbar^3p_F^5e^2}\frac{1}{H(\lambda)}\sum_{l',l}C_{ll'}A_l^sA_{l'}^s\ . \tag{59}$$

Here the coefficients $C_{ll'}$ are given by

$$C_{ll'}=\left\langle\{2P_l(q_1)P_{l'}(q_1)+[P_l(q_1)+P_l(q)][P_{l'}(q_1)+P_{l'}(q)]\}\frac{\sin^2(\theta/2)}{\cos(\theta/2)}\right\rangle . \tag{60}$$

We keep in mind that q_1 and q are functions of θ and ϕ, Eqs. (36) and (37).

Besides the resistivity, there are two other experimental quantities, the specific-heat capacity and the susceptibility, both of which can be parametrized by Landau coefficients. We now address the mass enhancement m^*/m_b, and the susceptibility enhancement χ/χ_0.

From the Galilean invariance, we get a general relation between the quasiparticle velocity and the Landau interaction function $f(\mathbf{p},\mathbf{p}')$.[46] The current is given by the equation

$$\mathbf{J}(\mathbf{p})=\mathbf{v}(\mathbf{p})+\sum_{\sigma'}\int\frac{d^3p'}{(2\pi)^3}f(\mathbf{p},\mathbf{p}')\delta(\varepsilon(\mathbf{p}')-\mu)\cdot\mathbf{v}(\mathbf{p}') . \tag{61}$$

Since we treat the conduction electrons as nearly free, neglecting periodic lattice effects such as umklapp scattering, the current is proportional to the momentum. Hence, Eq. (59) gives the relation

$$\mathbf{v}(\mathbf{p})=\frac{\mathbf{p}}{m_b}-\sum_{\sigma'}\int\frac{d^3p'}{(2\pi)^3}f(\mathbf{p},\mathbf{p}')\delta(\varepsilon(\mathbf{p}')-\mu)\cdot\mathbf{v}(\mathbf{p}')=\frac{\mathbf{p}}{m_b}-\sum_{\sigma'}\int\frac{d^3p'}{(2\pi)^3}a(\mathbf{p},\mathbf{p}')\delta(\varepsilon(\mathbf{p}')-\mu)\cdot\frac{\mathbf{p}'}{m_b} . \tag{62}$$

The solving kernel, $a(\mathbf{p},\mathbf{p}')$, is related to the scattering amplitude A, Eq. (43), and is the Neumann series of the Landau scattering function f; m_b is the band mass. Hence, for an isotropic system where the momentum is parallel to the velocity, we finally get the mass enhancement[47]

$$m^*/m_b=(1-\tfrac{1}{3}A_1^s)^{-1} . \tag{63}$$

In a similar manner the spin susceptibility is obtained as

$$\frac{\chi}{\chi_0}=\frac{m^*}{m_b}(1-A_0^a)=\frac{m^*}{m_b}(1+\tfrac{1}{3}A_0^s) . \tag{64}$$

From the measurement of the heat capacity, we have $m^*/m_b\simeq 4.5$, and hence get $A_1^s\simeq 2.3$. From the measurement of the spin susceptibility, we have $(\chi/\chi_0)/(m^*/m_b)\simeq 2$ and obtain $A_0^s\simeq 3.2$. A third coefficient, A_2, may be determined by the sum rule $\sum_l A_l=0$, Eq. (56), if we neglect all terms with $l\geq 3$; then $A_2=-5.5$.[48]

Taking into account the first two Landau coefficients, we calculate the resistivity coefficient A to be 0.034 $\mu\Omega\,\mathrm{cm/K^{-2}}$; we take $H(\lambda)$ to be 0.5 since $H(\lambda)$ is only a slowly varying function of λ. This value of A is in good agreement with the experimental value 0.042. Hence we obtain in a consistent manner—by fitting two parameters and evaluating a third quantity—good agreement with the experimental data. We conclude therefore, that the e_g electrons in V_2O_3 can be described as a Fermi liquid. If, in addition, we take into account A_2, then we find almost no change of A ($<1\%$).

We now proceed to evaluate on the basis of a microscopic theory the Landau coefficients A_l. Remembering that V_2O_3 is close to an antiferromagnetic transition, we take as an effective interaction J the interaction which arises from the exchange of the magnetic excitations,

$$\bar{J}(q)=\int\frac{d\Omega_{\mathbf{q}}}{4\pi}\frac{J^2\frac{1}{2}M(\mathbf{q})\chi_0}{1-J^2M(\mathbf{q})\chi_0\chi^e(q)} . \tag{65}$$

This equation assumes that $J(\mathbf{q})$ is replaced by the angular average, denoted $\bar{J}(\mathbf{q})$. In real solids, $J(\mathbf{q})$ is anisotropic due to the squared matrix element, $M(\mathbf{q})$, Eq. (24). Also, the Fermi surface is anisotropic. When the anisotropy of $J(\mathbf{q})$ is taken into account, one finds that the spin-fluctuation contribution depends on the states, $\mathbf{p}$ and $\mathbf{p}'$, at the Fermi surface; that is, it depends on $\mathbf{p}$ and on the direction of $\mathbf{p}-\mathbf{p}'$ with respect to the crystalline axes. Thus, a relation is obtained, Eq. (62), that holds at each of the different points $\mathbf{p}$ on the Fermi surface. By averaging over the directions of the momentum transfers in $J(\mathbf{q})$, we arrive at the quasi-isotropic model. The foregoing model assumption is equivalent to the neglect of all of the anisotropy coefficients in the expansion of $J(\mathbf{q})$ in terms of the harmonics for the trigonal V_2O_3 symmetry. These harmonics are of second and higher order in the direction cosines. On the other hand, the Landau coefficients for $l\geq 2$ cannot be determined from the experimental quantities C_v, χ, and ρ; the resistivity ρ is almost independent of the coefficients A_l, $1\geq 2$. As compared with the magnitude of Landau's coefficients A_2 in Table I, we expect that the lowest-anisotropy contributions are not very

TABLE I. Experimental and theoretical values of the Landau coefficients A_l.

	C_v	$(\chi/\chi_0)/(m^*/m_b)$	$A\left[\frac{\mu\Omega\,\mathrm{cm}^2}{\mathrm{K}^2}\right]$
Experimental values	$\frac{m^*}{m_b}=4.5$	2	0.042
	A_0	A_1	A_2
Experimental values	3.2	2.3	-5.5[a]
Theory			
$q_m=0.535$[b]	3.2	4.1	-3.6
$q_m=0.615$[c]	3.2	2.3	-6.5

[a]This value is determined by the sum rule $\sum_l A_l=0$.

[b]The parameter q_m gives the position of the peak of $\bar{J}(q)$ taking the cylindrical model for $\chi(q)$, cf. Fig. 9.

[c]This q_m gives the position of the peak of $\bar{J}(q)$ if one assumes that the electronic polarizability $\chi^e(q)$ is a constant in the region of short wavelengths.

relevant. The reason for A_2 being rather large, as is consistent with the sum rule (cf. Table I), is the quasisingular behavior of $\bar{J}(q)$, cf. Fig. 9. Hence, by averaging $J(\mathbf{q})$ over all $\mathbf{q}$ directions and by treating the e_g electrons as an isotropic quasiparticle system, we are consistent within our model.

Substituting the $\bar{J}(q)$, in Eq. (54), we obtain for the coefficients A_l^s the result

$$A_l^s=\frac{3(2l+1)}{2(m^*/m_b)} \times\int\frac{d\Omega_q}{4\pi}\int_0^1 dq\, q\frac{WF(\mathbf{q})}{1-W\tilde{\chi}(\mathbf{q})F(\mathbf{q})}P_l(1-2q^2)\,. \tag{66}$$

The quantities $\tilde{\chi}$ and $F(q)$ are defined by Eqs. (B5) and (B6); q is normalized with respect to $2p_F$.

In the effective-potential model we can evaluate the parameters $A_l^{s,a}$ by fitting the interaction parameter W to A_0. In order to explain the magnitude of A_0, we observe that the spectral function

$$S(q)=\int\frac{d\Omega_q}{4\pi}\frac{WF(\mathbf{q})}{1-W\tilde{\chi}(q)F(\mathbf{q})} \tag{67}$$

has to be nearly 1 order of magnitude larger than the corresponding quantity occurring in Eq. (B7) which is used to evaluate the effective mass. This requires that the interaction parameter W be very close to its limiting value, W_0, where the system becomes unstable against the antiferromagnetic transition.

Unfortunately, the experiments yield only the first two Landau parameters. Hence, we cannot reconstruct the q dependence of the effective potential. However, we get some further information about $\bar{J}(q)$ by looking at the ratio A_0/A_1. Assuming the cylindrical model, Sec. III, in Fig. 9 we plot for the parameter value $W=1.128$. It is seen that this function has a steep peak at q_m, where q_m is determined by the maximum of the denominator function $\tilde{\chi}(q)F(\mathbf{q})$ in Eq. (67). The weight of $S(q)$ increases strongly as W approaches W_0. Then, the ratio A_0/A_1 is, to a very good approximation, given by

$$\frac{A_0}{A_1}\simeq\frac{1}{3P_1(1-2q_m^2)}\,. \tag{68}$$

From the experimentally observed ratio A_0/A_1, we conclude that the maximum of the function $S(q)$ should be near $q_m\simeq 0.615$. When compared with the previously found value of $q_m\simeq 0.535$, the agreement is satisfactory. If we would take $\tilde{\chi}$ to be independent of q, the maximum would occur at $q_m\simeq 0.615$. The main conclusion is that one needs a sufficiently large phase-space volume in the $\mathbf{q}$ space, where the nearly singular behavior of the effective potential occurs; this potential should have a strong peak close to $q\simeq 0.615$, cf. Table I. It appears that the metal-insulator transition is a magnetic transition driven by the exchange interaction between the e_g electrons, whereby the shape of the Fermi surface—and the existence of some nesting parts—should provide sufficient phase space in order to drive the antiferromagnetic instability.

The approximation of the local potential model, namely taking into account only the exchange interaction due to the magnetic excitations, results, however, in a serious deficiency: $A_0^s>1$. A Fermi liquid with $A_0^2>1$ or $F_0^s<-1$ becomes unstable to fluctuations in the density. A hint of how to resolve this problem is given by the work of Ainsworth *et al.*[49] These authors point out the importance of the *direct* electron-electron interaction. The inclusion of this interaction yields more reasonable values of the Landau parameters F_l and a better convergence of the F_l series. The model in which the direct interaction is assumed to be of zero range (e.g., the Stoner model) is not sufficient to obtain reasonable values for the A_l. In order to include both the direct interaction and the induced interaction, we add, as in Refs. 40 and 41, the effective interaction $j(q)$ (Ref. 50) to our exchange potential $J(q)$, Eq. (32). The behavior of $j(q)$ near $q\approx 0$ is well described by the paramagnon model. However, for larger values of q there are deviations from the simple model potentials used in Ref. 40. First of all, the direct exchange interaction has a finite range, resulting in a q dependence. As discussed by Herring[51] and Schrieffer,[52] this momentum dependence cannot be neglected in order to get reasonable results in paramagnetic metals. Herring argues that the main contribution to the exchange interaction near $q\approx 0$ arises from the interaction of charge distributions on *different* atoms. Although the matrix elements of these interactions are smaller than the one-center integrals, the summation over the nearest neighbors causes these two-center integrals to be the dominant ones near $\mathbf{q}=\mathbf{k}-\mathbf{k}'\approx 0$. Hence, it is obvious that there are negative contributions to $j(q)$ by virtue of the two-center integrals. An additional source of the q dependence of the direct interaction is the exchange of two or more spin fluctuations.[53] In view of the fact that there exist so far no quantitative calculations of the q dependence of the exchange interaction between d electrons, we fit the effective potential $j(q)$ by experiment.

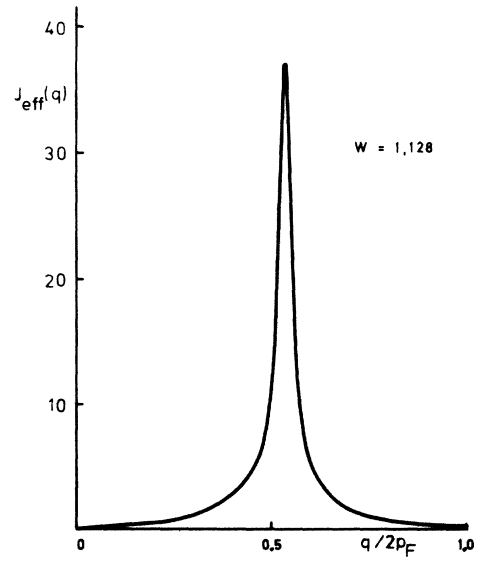

FIG. 9. Plot of the effective potential $\bar{J}(q)$ vs $q/2p_F$.

Including $j(q)$, the equations of this section remain unchanged, except that we replace the Eqs. (54) and (55) by

$$A_0^s=\tfrac{3}{2}(j_0+J_0)\ , \tag{69}$$

$$A_0^a=-j(0)-\tfrac{1}{2}(j_0+J_0)\ , \tag{70}$$

$$A_l^s=\tfrac{3}{2}(j_l+J_l),\quad l\geq 1 \tag{71}$$

$$A_l^a=-\tfrac{1}{2}(j_l+J_l),\quad l\geq 1 \tag{72}$$

where $j(0)=\sum_l j_l$. Hence, the forward-scattering sum rule is satisfied. In the following we include all terms with $l\leq 2$.

Using the relation

$$J_l=(2l+1)P_l(1-2q_m^2)J_0\ ,$$

corresponding to Eq. (68), we determine q_m from the sum rule, $\sum_l J_l=0$. The result is $q_m=0.596$, in good agreement with the value found in our model for $J(q)$ by assuming $\tilde{\chi}$ to be independent of q. Hence, we find $J_1=\alpha J_0$, $J_2=-(1+\alpha)J_0$ with $\alpha=0.87$. We are left with a single adjustable parameter, J_0.

Because of the stability of the metallic phase of V_2O_3, we have $A_0^s<1$. On the other hand, this phase is close to the metal-insulator transition. Hence, the choice $A_0^s\cong 0.95$ is appropriate for the metallic phase of V_2O_3. From the experimental values, $A_0^a=-1.06$ and $A_1^s=2.3$, we find $j(0)=0.743$. Using the forward-scattering sum rule we get $A_2^s=-2.1$. Hence, we have the following equations for determining the potential $j(q)$:

$$j_0+J_0=-2[A_1^a+j(0)]=0.633\ , \tag{73}$$

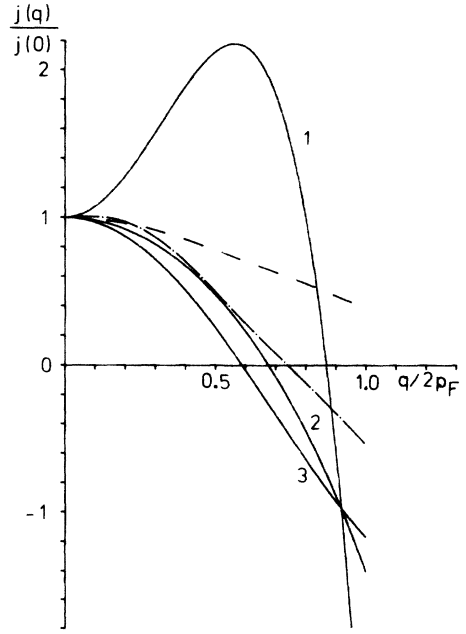

FIG. 10. Effective potential $j(q)$ describing the electron interaction between the e_g electrons. The potentials for ^{3}He (—·—·—·) and for a Stoner model (— — —) [$j(q)=Z^{-1}I(1-I\chi)$, where $I=0.76$ is determined from $j(0)$] are shown for comparison. The solid lines 1,2,3 correspond to the parameters $J_0=0$, $j_0=-0.1$, and $j_0=-0.2$, respectively.

$$j_1+\alpha J_0=\tfrac{2}{3}A_1^s=1.53\ , \tag{74}$$

$$j_2-(1+\alpha)J_0=\tfrac{2}{3}A_2^s=-1.42\ . \tag{75}$$

Given the quantity j_0 or J_0, we can determine the potential

$$j(q)=\sum_l j_l P_l(1-2q^2)\ .$$

As seen in Fig. 10, the choice of $J_0=0$ leads to an effective potential which has a maximum at a finite value of q, indicating the antiferromagnetic behavior of the metallic phase. Hence, the inclusion of the antiferromagnetic exchange interaction, $J(q)\neq 0$, yields a more reasonable potential, $j(q)$, for the direct interaction. The choice of $j_0\approx -0.1$ yields a reasonable approximation for $j(q)$, as seen from Fig. 10. The behavior of $j(q)$ differs from the simple paramagnon model for large values of q. This behavior is similar to that found in ^{3}He. Since we are far away from the ferromagnetic limit, the behavior of $j(q)$ at larger values of q becomes more important in averaging the potential with Legendre polynomials [cf. comments above Eq. (69)].

Taking into account the potential $j(q)$ in addition to the dominant antiferromagnetic potential $J(q)$, we obtain smaller values for $J(q)$. This implies that the interaction parameter W is not as close to the instability point W_0 as in the absence of $j(q)$. With the new choice of the A_l the result for the resistivity coefficient A does not change appreciably. Equation (58) remains valid, except for replacing A_0^s by $A_0^s+\frac{3}{2}j(0)$. This value is 2.07, as compared to the value $A_0^s=2.3$ for $j(q)=0$. Hence, the resistivity coefficient A decreases only slightly and is still in good agreement with experiment.

V. SUMMARY AND CONCLUSIONS

It is shown that the concept of antiferromagnetic spin fluctuations plays an important role for the understanding of the unusual d-band properties of metallic V_2O_3. The spin fluctuations consist here of molecular magnetic excitations of the two coupled, vertical V_2 pairs (Fig. 2) that form the metallic basis of the trigonal unit cell. The fluctuations are due to transitions of the a_{1g} electrons localized at the V_2 pairs. The correlation effects between the a_{1g} electrons are caused by the short-range Coulomb interactions and are treated with Hubbard's Hamiltonian for the two V_2 pairs. It is found in Sec. II that the lowest excited state is a spin-triplet state lying close to the ground-state singlet. The virtual singlet-triplet excitations of the a_{1g} electrons, i.e., the molecular magnetic polarizability of the two V_2 pairs in a unit cell gives rise to an interaction between the remaining conduction (e_g) electrons. A first e_g electron polarizes the singlet state formed by the two a_{1g} electrons per V_4 molecule and thereby affects the motion of a second e_g electron. The corresponding dynamic susceptibility of the conduction electrons is found with a RPA calculation; the results are given by Eqs. (21) and (23) of Sec. III. We then proceed to evaluate the electron mass renormalization due to the virtual emission and reabsorption of the local magnetic excitations, in analogy with the ordinary paramagnon theory for strong-

ly *paramagnetic* metals.[54] We find that both the effective mass and the electron-electron scattering amplitude, as measured by the T^2 coefficient of the electrical resistivity ρ, diverge as the system approaches the antiferromagnetic instability, Figs. 6 and 7. As the mass is enhanced, the particles become immobile and tend to localize.

This localization is different from the Brinkman-Rice concept. In their theory, the primary effect of the Coulomb repulsion is to keep the electrons apart, at their lattice sites, in order to avoid a double occupancy (in the case of a half-filled band). However, in the context of antiferromagnetic spin fluctuations and the metal-insulator transition, we should mention that our model does not yet give a realistic description of the *M-I* transition. The reason is that we neglect real band-structure effects of the e_g electrons such as the shape of the Fermi surface and—what is more important—the detailed form of the susceptibility function. Because of a lack of a band theory for the susceptibility function, we use the Lindhard function. However, as is well known from, e.g., Cr, the structure of this function in momentum space plays an important role in antiferromagnetic band transitions.[55] Usually, the phase transition is attributed to some structure of this function at short wave lengths. Of comparable importance is the $\mathbf{q}$ dependence of the form factors, i.e., the matrix element $M(\mathbf{q})$, as discussed in Sec. III.

In Sec. IV we viewed the e_g electrons as a Fermi liquid. The basic reason for this attempt is the fact that an e_g electron can be viewed as a Landau quasiparticle, the effective mass of which is larger than the band mass by a factor 4—5, by virtue of its interaction with the localized spin fluctuations, Sec. III. These excitations also give rise to an effective interaction among the quasiparticles. We do not believe that phonons play a dominant role in the mass enhancement; otherwise metallic V_2O_3 could become an ordinary BCS superconductor at a reasonably high temperature and not an antiferromagnetic insulator.

At this time an exact formulation of the Fermi-liquid theory for real solids is lacking that takes into account the crystal symmetry, i.e., the periodic lattice and the anisotropy effects. This observation, however, has not hindered the successful Fermi-liquid description of the electron-phonon system of simple metals, despite the large phonon-anisotropy effects.[56] We therefore attempt to apply the isotropic Fermi-liquid theory to V_2O_3. The basic approximation (Sec. IV) consists of approximating the static vertex function of Landau's theory by an effective scattering potential. The physical origin of this short-range potential is the exchange of the magnetic excitations discussed in Sec. III. By taking an angular average of the potential, we are consistent with the Galilean invariance of the ideal system.[46] Furthermore, the anisotropic effect of the matrix element $M(\mathbf{q})$, Eq. (24), appears to be small for the Landau parameters with $l<2$, for reasons similar to the small effect of the anisotropic electron-phonon matrix element on these parameters for simple metals. In addition to the potential $J(q)$, we include the usual effective interaction between the conduction electrons in order to have a stable Fermi liquid, cf. Eqs. (69)—(72). We find that the isotropic antiferromagnetic spin-fluctuation model of Sec. IV yields a consistent quasiparticle description of the metallic properties, C_v, χ, and ρ, for V_2O_3.

Recently, an attempt was made to apply the Fermi-liquid description to the "heavy fermions" in $CeCu_2Si_2$.[37,57] Although the effective mass and the T^2 coefficient of ρ of V_2O_3 are not as large as in $CeCu_2Si_2$, there are similarities between the local excitations giving rise to the interaction. The Ce^{3+} ion allows for many-electron excited states involving *other* (i.e., conduction) electrons besides its *own* four f electrons, whereas at the V_2 pairs only the local a_{1g} electrons participate in the magnetic excitations. Just $CeCu_2Si_2$ or other rare-earth compounds, pure V_2O_3 could be an interesting candidate for triplet superconductivity, as was recently mentioned by Anderson. So far, superconductivity is not observed down to 0.3 K. Whether or not superconductivity can occur in V_2O_3 is under investigation.

ACKNOWLEDGMENTS

It is a pleasure to thank Professor J. M. Honig for many interesting discussions on V_2O_3 and Dr. M. Grodzicki for his help concerning the electronic structure of the metallic phase. We would like to thank Professor S. Werner for communicating the results of his neutron scattering experiments and Professor D. Fay for a critical reading of the manuscript. The support of this work through the Deutsche Forschungsgemeinschaft (Bonn, Germany) is gratefully acknowledged.

APPENDIX A

In Table II we give the eigenvalue spectrum for the V_4 molecule.

The Hartree-Fock energies (eV) and Hartree-Fock eigenfunctions for the states S_1, S_3, S_7, and S_8 are tabulated in the following for comparison with the exact results, cf. Table I:

$$S_1:\ -2(a+b)+U/4=-1.825\ ,\ \tfrac{1}{2}(\phi_0+\phi_1+\phi_2+\phi_3)\ ,$$

$$S_3:\ -2(a-b)+U/4=-0.865\ ,\ \tfrac{1}{2}(\phi_0+\phi_1-\phi_2-\phi_3)\ ,$$

$$S_7:\ 2(a-b)+U/4=1.615\ ,\ \tfrac{1}{2}(-\phi_0+\phi_1-\phi_2+\phi_3)\ ,$$

$$S_{10}:\ 2(a+b)+U/4=2.625\ ,\ \tfrac{1}{2}(\phi_0-\phi_1-\phi_2+\phi_3)\ .$$

APPENDIX B

We calculate the contributions of the transverse magnetic excitations to $\partial\Sigma/\partial\omega$, determined by χ^{+-}, using the standard procedure ($\omega\to 0$):

$$\frac{\partial\Sigma}{\partial\omega}=-J^2N(0)\int\frac{d\Omega(\theta,\phi)}{8\pi}\chi^{+-}(p_F,\theta_0,\phi_0;p_F,\theta,\phi)\ . \tag{B1}$$

The z axis is fixed and oriented parallel to the c axis. The integration $\int d\cos\theta\int d\phi$ can be written as

$$\int d\cos\theta\int d\phi=\frac{2}{p_F}\int d^3\mathbf{p}\,\delta(p^2-p_F^2)\ . \tag{B2}$$

Hence, we obtain

TABLE II. Spectrum of the V_4 molecule. The parameters are $U=1.5$ eV, $a=0.86$ eV, $b=0.24$ eV, and $t=0$.

Type: Singlet (S) Triplet (T)	Energy (eV)	Eigenfunctions
S_1 ($\equiv S$)	-1.98	$0.279\phi_0+0.394\phi_1+0.611\phi_2+0.626\phi_3$[a]
T_1 ($\equiv T$)	$-2a=-1.72$	$\frac{1}{2}(c_{1\uparrow}^\dagger+c_{2\uparrow})(c_{3\uparrow}^\dagger c_{4\uparrow}^\dagger)\vert 0\rangle$[b]
S_2	$\frac{1}{2}[U-(U^2+16a^2)^{1/2}]=-1.12$	$\frac{1}{2N}\left[c_{1\uparrow}^\dagger c_{2\downarrow}^\dagger+c_{2\uparrow}^\dagger c_{1\downarrow}^\dagger-c_{3\uparrow}^\dagger c_{4\downarrow}-c_{4\uparrow}^\dagger c_{3\downarrow}^\dagger+\frac{-U+(U^2+16a^2)^{1/2}}{4a}\times(c_{1\uparrow}^\dagger c_{1\downarrow}^\dagger+c_{2\uparrow}^\dagger c_{2\downarrow}^\dagger-c_{3\uparrow}^\dagger c_{3\downarrow}^\dagger-c_{4\uparrow}^\dagger c_{4\downarrow}^\dagger)\right]\vert 0\rangle$[c]
S_3	-0.871	$0.464\phi_0+0.742\phi_1-0.367\phi_2-0.315\phi_3$
T_2	$-2b=-0.48$	$\frac{1}{2}(c_{1\uparrow}^\dagger+c_{4\uparrow}^\dagger)(c_{2\uparrow}^\dagger+c_{3\downarrow}^\dagger)\vert 0\rangle$
S_4	$\frac{1}{2}[U-(U^2+16b^2)^{1/2}]=-1.40$	$\frac{1}{2N}\left[c_{1\uparrow}^\dagger c_{4\downarrow}^\dagger+c_{4\uparrow}^\dagger c_{1\downarrow}^\dagger-c_{2\uparrow}^\dagger c_{3\downarrow}^\dagger-c_{3\uparrow}^\dagger c_{2\downarrow}^\dagger+\frac{-U+(U^2+16b^2)^{1/2}}{2b}\times(c_{1\uparrow}^\dagger c_{1\uparrow}^\dagger+c_{4\uparrow}^\dagger c_{4\uparrow}^\dagger-c_{3\uparrow}^\dagger c_{3\uparrow}^\dagger-c_{2\uparrow}^\dagger c_{2\uparrow}^\dagger)\right]\vert 0\rangle$
S_5	0	$\frac{1}{2}(c_{1\uparrow}^\dagger c_{3\downarrow}^\dagger+c_{3\uparrow}^\dagger c_{1\downarrow}^\dagger-c_{2\uparrow}^\dagger c_{4\downarrow}^\dagger-c_{4\uparrow}^\dagger c_{2\downarrow}^\dagger)\vert 0\rangle$
T_3	0	$\frac{1}{2}(c_{1\uparrow}^\dagger+c_{3\uparrow}^\dagger)(c_{2\uparrow}^\dagger+c_{4\uparrow}^\dagger)\vert 0\rangle$
T_4	0	$\frac{1}{2}(c_{1\uparrow}^\dagger-c_{3\uparrow}^\dagger)(c_{2\uparrow}^\dagger-c_{4\uparrow}^\dagger)\vert 0\rangle$
T_5	$2b=0.48$	$\frac{1}{2}(c_{1\uparrow}^\dagger-c_{4\uparrow}^\dagger)(c_{3\uparrow}^\dagger-c_{2\uparrow}^\dagger)\vert 0\rangle$
S_6	$U=1.5$	$\frac{1}{2}(c_{1\uparrow}^\dagger c_{1\downarrow}^\dagger-c_{2\uparrow}^\dagger c_{2\downarrow}^\dagger+c_{3\uparrow}^\dagger c_{3\downarrow}^\dagger-c_{4\uparrow}^\dagger c_{4\downarrow}^\dagger)\vert 0\rangle$
S_7	1.524	$-0.347\phi_0+0.183\phi_1-0.638\phi_2+0.662\phi_3$
S_8	$\frac{1}{2}[U+(U^2+16b^2)^{1/2}]=-1.64$	$\frac{1}{2N}\left[c_{1\uparrow}^\dagger c_{4\downarrow}^\dagger+c_{4\uparrow}^\dagger c_{1\downarrow}^\dagger-c_{2\uparrow}^\dagger c_{3\downarrow}^\dagger-c_{3\uparrow}^\dagger c_{2\downarrow}^\dagger-\frac{U+(U^2+16a^2)^{1/2}}{4a}\times(c_{1\uparrow}^\dagger c_{1\downarrow}^\dagger-c_{2\uparrow}^\dagger c_{2\downarrow}^\dagger-c_{3\uparrow}^\dagger c_{3\downarrow}^\dagger+c_{4\uparrow}^\dagger c_{4\downarrow}^\dagger)\right]\vert 0\rangle$
T_6	$2a=1.72$	$\frac{1}{2}(c_{1\uparrow}^\dagger-c_{2\uparrow}^\dagger)(c_{3\uparrow}^\dagger-c_{4\uparrow}^\dagger)\vert 0\rangle$
S_9	$\frac{1}{2}[U+(U^2+16a^2)^{1/2}]=-2.621$	$\frac{1}{2N}\left[c_{1\uparrow}^\dagger c_{2\downarrow}^\dagger+c_{2\uparrow}^\dagger c_{1\downarrow}^\dagger-c_{3\uparrow}^\dagger c_{4\downarrow}-c_{4\uparrow}^\dagger c_{3\downarrow}^\dagger-\frac{U+(U^2+16a^2)^{1/2}}{4a}\times(c_{1\uparrow}^\dagger c_{1\downarrow}^\dagger+c_{2\uparrow}^\dagger c_{2\downarrow}^\dagger-c_{3\uparrow}^\dagger c_{3\downarrow}^\dagger-c_{4\uparrow}^\dagger c_{4\downarrow}^\dagger)\right]\vert 0\rangle$
S_{10}	2.828	$0.765\phi_0-0.51\phi_1-0.289\phi_2+0.263\phi_3$

[a]The eigenfunctions ϕ_i are defined in Sec. II.

[b]We have written only the triplet state that is of the type $\frac{1}{2}A_\uparrow B_\uparrow$. The other triplet states are given by $(1/2\sqrt{2})(A_\uparrow^\dagger B_\downarrow^\dagger+A_\downarrow^\dagger B_\uparrow^\dagger)$ and $\frac{1}{2}A_\uparrow^\dagger B_\downarrow^\dagger$.

[c]N is the normalization constant.

$$\int\frac{d\Omega}{4\pi}\frac{\partial\Sigma}{\partial\omega}=-J^2N(0)\frac{1}{4\pi^2p_F^2}\int d^3\mathbf{p}\int d\mathbf{q}^3\,\delta(p^2-p_F^2)\delta((\mathbf{p}-\mathbf{q})^2-p_F^2)\chi^{+-}(\mathbf{q})$$
$$=-J^2N(0)\frac{1}{4\pi}\int d^3\mathbf{q}\frac{1}{q}\chi^{+-}(\mathbf{q})\Theta(1-q)\,, \tag{B3}$$

where in the last term q is normalized with respect to $2p_F$. It is convenient to define the dimensionless parameter W,

$$W=\tfrac{1}{4}(\eta_1+\eta_2)^2J^2N(0)\chi_0(0)\,, \tag{B4}$$

where $\chi_0(0)=2/\Delta$, and to introduce the functions

$$\tilde{\chi}(\mathbf{q})=\left[\frac{1}{2}+\frac{1-q^2}{4q}\ln\left[\frac{1+q}{1-q}\right]\right], \tag{B5}$$

$$F(\mathbf{q})=M(\mathbf{q})[\tfrac{1}{4}(\eta_1+\eta_2)^2]$$
$$=[\cos(q_zD_{12})\sin(q_xD_{23}-q_zD_{12})]^2\,. \tag{B6}$$

Here, $D_{12}=p_F d_{12}$ and $D_{23}=p_F d_{23}$. We write Eq. (B3) in terms of these variables and get

$$\int \frac{d\Omega}{4\pi}\frac{\partial\Sigma}{\partial\omega} = -\frac{1}{4\pi}\int d^3\mathbf{q}\,\Theta(1-q)\frac{WF(\mathbf{q})}{1-WF(\mathbf{q})\tilde{\chi}(\mathbf{q})}\frac{1}{q} . \tag{B7}$$

Since the main contribution to the integral comes from the pole, and $F(\mathbf{q})$ is a rapidly varying function of $\mathbf{q}$ in comparison with $\tilde{\chi}(\mathbf{q})$, we approximate $\tilde{\chi}(\mathbf{q})$ by the constant value

$$\tilde{\chi}_c=\tilde{\chi}(\mathbf{q}=(\pi/D_{23},0,0)) .$$

The q_y integration is now easily performed. Introducing the polar coordinates for q_z and q_x, we finally obtain

$$\int \frac{d\Omega}{4\pi}\frac{\partial\Sigma}{\partial\omega} = -\frac{1}{2\pi}\int_0^1 dq\,q\ln\left|\frac{1+(1-q^2)^{1/2}}{1-(1-q^2)^{1/2}}\right| \times\int_0^\pi d\phi\frac{WF(q,\phi)}{1-WF(q,\phi)\tilde{\chi}} . \tag{B8}$$

This expression is evaluated numerically.

In order to evaluate the T^2 coefficient A of the resistivity, we use the relation

$$\lim_{\omega\to 0}\left[\frac{\mathrm{Im}\chi^{+-}(\mathbf{q},\omega)}{\omega}\right] = \frac{J^2[\chi_0(0)M(\mathbf{q})]^2}{[1-J^2\chi_0(0)M(\mathbf{q})\chi^e(\mathbf{q},0)]^2}\frac{m_b^2}{4\pi q} . \tag{B9}$$

Then we obtain A in an analogous procedure; the result is

$$A=\frac{3\pi^4 m_b^2 k_B^2}{e^2 p_F^2}\frac{1}{8}\int d^3q\,\Theta(1-q)\left[\frac{WF}{1-WF\tilde{\chi}}\right]^2 . \tag{B10}$$

If we again approximate $\tilde{\chi}(q)$ by the constant $\tilde{\chi}_c$, we may perform the q_y integration and get

$$A=\frac{3\pi^4}{2}\frac{k_B^2}{e^2}\frac{m_b^2}{p_F^5}\int_0^1 dq\,q(1-q^2)^{1/2} \times\int_0^\pi d\phi\frac{W^2F^2(q,\phi)}{[1-WF(q,\phi)\tilde{\chi}]^2} . \tag{B11}$$

[1]N. F. Mott, Rev. Mod. Phys. **40**, 677 (1968).
[2]W. Kohn, Phys. Rev. Lett. **19**, 789 (1967).
[3]D. Adler, Rev. Mod. Phys. **40**, 714 (1968).
[4]H. J. Zeiger, Phys. Rev. B **11**, 5132 (1975).
[5]M. Weger, Philos. Mag. **24**, 1095 (1971).
[6]J. Ashkenazi and M. Weger, Adv. Phys. **73**, 207 (1973).
[7]T. M. Rice and W. B. Brinkman, Phys. Rev. B **2**, 4302 (1970); M. C. Gutzwiller, Phys. Rev. **137**, A1726 (1965).
[8]W. F. Brinkman and T. M. Rice, Phys. Rev. B **5**, 4350 (1972).
[9]T. M. Rice and D. B. McWhan, IBM J. Res. Dev. **14**, 251 (1970).
[10]D. B. McWhan, A. Menth, J. P. Remeika, W. F. Brinkman, and T. M. Rice, Phys. Rev. B **7**, 1920 (1973). Here, references are given to the experimental work at Bell Laboratories.
[11]J. M. Honig, L. L. van Zandt, R. D. Board, and H. E. Weaver, Phys. Rev. B **6**, 1323 (1972).
[12]H. Kuwamoto, J. M. Honig, and J. Appel, Phys. Rev. B **22**, 2626 (1982).
[13]C. Castellani, C. R. Natoli, and J. Ranninger, Phys. Rev. B **18**, 4945 (1978).
[14]C. Castellani, C. R. Natoli, and J. Ranninger, Phys. Rev. B **18**, 4967 (1978).
[15]C. Castellani, C. R. Natoli, and J. Ranninger, Phys. Rev. B **18**, 5001 (1978). Compare Ref. 10, p. 1930.
[17]J. M. Honig (private communication).
[18]D. Vollhardt, Rev. Mod. Phys. **56**, 99 (1984).
[19]A. W. Overhauser, Phys. Rev. **128**, 1437 (1962).
[20]W. M. Lomer, Proc. Phys. Soc. London **80**, 489 (1962).
[21]T. M. Rice, Phys. Rev. B **2**, 3619 (1970).
[22]D. B. McWhan, J. P. Remeika, S. D. Bader, B. B. Triplett, and N. E. Phillips, Phys. Rev. B **7**, 3097 (1972).
[23]D. B. McWhan, J. P. Remeika, T. M. Rice, W. F. Brinkman, J. P. Maita and A. Menth, Phys. Rev. Lett. **27**, 941 (1971).
[24]M. Grodzicki and O. Jepsen (unpublished).
[25]A. Menth and J. P. Remeika, Phys. Rev. B **2**, 3756 (1970).
[26]D. B. McWhan and J. P. Remeika, Phys. Rev. B **2**, 3734 (1970).
[27]D. B. McWhan and T. M. Rice, Phys. Rev. Lett. **22**, 887 (1969).
[28]K. Andres, J. E. Graebner, and H. R. Ott, Phys. Rev. Lett. **35**, 1779 (1975).
[29]P. W. Anderson, Phys. Rev. B **30**, 1549 (1984).
[30]N. F. Mott (private communication).
[31]Y. Ueda, K. Kosuge, and S. Kachi, J. Solid State Chem. **31**, 171 (1980).
[32]J. Ashkenazi and T. Cuchem, Philos. Mag. **32**, 763 (1975).
[33]L. M. Falicov and R. A. Harris, J. Chem. Phys. **51**, 3153 (1969).
[34]R. M. White and P. Fulde, Phys. Rev. Lett. **47**, 1540 (1981).
[35]W. B. Yelon, S. A. Werner, S. Shivashankar, and J. M. Honig, Phys. Rev. B **24**, 1818 (1981); S. A. Werner, R. E. Word, W. B. Yelon, J. M. Honig, and S. Shivashankar, J. Appl. Phys. **52**, 2237 (1981); Phys. Rev. B **23**, 3533 (1981).
[36]P. Hertel, J. Appel, and D. Fay, Phys. Rev. B **22**, 534 (1980).
[37]F. Steglich, J. Aarts, C. D. Bredl W. Liebe, D. Meschede, W. Franz, and H. Schäfer, Phys. Rev. Lett. **43**, 1982 (1979).
[38]H. R. Ott, H. Rüdiger, Z. Fisk, and J. L. Smith, Phys. Rev. Lett. **50**, 1595 (1983).
[39]L. E. DeLong, J. G. Huber, K. N. Yang, and M. B. Maple, Phys. Rev. Lett. **51**, 312 (1983).
[40]K. Levin and O. T. Valls, Phys. Rep. **98**, 1 (1983); we note that Eq. (2.3a) in this paper is not correct, as there is missing a density of states factor, $(N^*)^{-2}$. A. Layzer and D. Fay, Int. J. Magn. **1**, 135 (1971).
[41]J. A. Sauls and J. W. Serene, Phys. Rev. B **183**, (1981).
[42]J. W. Serene and D. Rainer, Phys. Rep. **101**, **221**, (1983).
[43]A. M. Dyugaev, Sov. Phys.—JETP **43**, 1247 (1976).
[44]As a further approximation, we neglect the exchange of density fluctuations in the effective potential. In a charged system these long-range interactions are present. If we include these

contributions, then the relation between the symmetric and antisymmetric Landau coefficients, Eq. (57), is no longer valid, and the number of Landau coefficients increases. However, near the antiferromagnetic instability the dominant contribution to the effective potential comes from the exchange of antiferromagnetic spin waves. Compared to this contribution the contributions of the density fluctuations can be neglected in a first approximation.

[45]K. S. Dy and C. J. Pethick, Phys. Rev. **185**, 373 (1969).

[46]D. Nozières, *Interacting Fermi Systems* (Benjamin, New York, 1964).

[47]The relationship between m^* and A_1^s does not depend on Galilean invariance. This is simply a Ward identity. D. Pines and D. Nozières, *The Theory of Quantum Liquids* (Benjamin, New York, 1966), Vol. I, p. 195.

[48]The convergence of the Landau coefficients with $l \geq 3$ is poor due to the fact that the main contributions in evaluating A_l come from the sharp peak structure of $J(q)$; cf. Fig. 9. These coefficients play a subordinate role for the experimental quantities discussed in the present paper.

[49]T. L. Ainsworth, K. S. Bedell, G. E. Brown, and K. F. Quader, J. Low Temp. Phys. **50**, 319 (1983).

[50]The scattering potentials $v(q)$ and $j(q)$ introduced in Ref. 40 describe the direct, the density, and the spin-density fluctuation contributions to the interaction. Since $v(q)$ is nearly constant and since all pairs of potentials v,j and v',j' which are related by $v'(q)=v(q)+3c$ and $j'(q)=j(q)+c$ yield the same scattering amplitude, we choose c in such a manner that $v(0)$ is zreo and the effect of v is included in $j(q)$.

[51]C. Herring, in *Magnetism*, edited by G. T. Rado and H. Suhl (Academic, New York, 1966), Vol. IV, Chaps. IX and X.

[52]J. R. Schrieffer, J. Appl. Phys. **39**, 642 (1968).

[53]S. Babu and G. E. Brown, Ann. Phys. (Leipzig) **78**, 1 (1973).

[54]N. F. Berk and J. R. Schrieffer, Phys. Rev. Lett. **17**, 433 (1966).

[55]T. M. Rice, Phys. Rev. B **2**, 3619 (1970).

[56]W. F. Brinkman, P. M. Platzmann, and T. M. Rice. Phys. Rev. **174**, 495 (1968).

[57]H. R. Ott, H. Rudigier, T. M. Rice, K. Ueda, Z. Fisk, and J. L. Smith, Phys. Rev. Lett. **52**, 1915 (1984).